PD-1 Blockade Expands Intratumoral Memory T Cells

Ribas, Antoni; Shin, Daniel Sanghoon; Zaretsky, Jesse; Frederiksen, Juliet Wairimu; Cornish, Andrew; Avramis, Earl; Seja, Elizabeth; Kivork, Christine; Siebert, Janet; Kaplan-Lefko, Paula

Total number of authors:
17

Published in:
Cancer Immunology Research

Link to article, DOI:
10.1158/2326-6066.CIR-15-0210

Publication date:
2016

Document Version
Publisher's PDF, also known as Version of record

Published OnlineFirst January 19, 2016; DOI: 10.1158/2326-6066.CIR-15-0210

Research Article

Cancer Immunology Research

PD-1 Blockade Expands Intratumoral Memory T Cells

Antoni Ribas[1,2,3,4], Daniel Sanghoon Shin[1], Jesse Zaretsky[1], Juliet Frederiksen[5], Andrew Cornish[6], Earl Avramis[1], Elizabeth Seja[1], Christine Kivork[1], Janet Siebert[7], Paula Kaplan-Lefko[1], Xiaoyan Wang[8], Bartosz Chmielowski[1], John A. Glaspy[1], Paul C. Tumeh[3,4,9], Thinle Chodon[10], Dana Pe'er[6], and Begoña Comin-Anduix[2,4]

Abstract

Tumor responses to programmed cell death protein 1 (PD-1) blockade therapy are mediated by T cells, which we characterized in 102 tumor biopsies obtained from 53 patients treated with pembrolizumab, an antibody to PD-1. Biopsies were dissociated, and single-cell infiltrates were analyzed by multicolor flow cytometry using two computational approaches to resolve the leukocyte phenotypes at the single-cell level. There was a statistically significant increase in the frequency of T cells in patients who responded to therapy. The frequency of intratumoral B cells and monocytic myeloid-derived suppressor cells significantly increased in patients' biopsies taken on treatment. The percentage of cells with a regulatory T-cell phenotype, monocytes, and natural killer cells did not change while on PD-1 blockade therapy. $CD8^+$ memory T cells were the most prominent phenotype that expanded intratumorally on therapy. However, the frequency of $CD4^+$ effector memory T cells significantly decreased on treatment, whereas $CD4^+$ effector T cells significantly increased in nonresponding tumors on therapy. In peripheral blood, an unusual population of blood cells expressing CD56 was detected in two patients with regressing melanoma. In conclusion, PD-1 blockade increases the frequency of T cells, B cells, and myeloid-derived suppressor cells in tumors, with the $CD8^+$ effector memory T-cell subset being the major T-cell phenotype expanded in patients with a response to therapy. *Cancer Immunol Res; 4(3); 194–203. ©2016 AACR.*

Introduction

The programmed cell death protein 1 (PD-1) is an immune checkpoint protein expressed in T cells. PD-1 inhibits T-cell responses to cancer after binding to one of its ligands, PD-1 ligand 1 (PD-L1 or B7-H1) or PD-L2 (also called B2-DC; refs. 1–4). PD-1 limits the activity of T cells by inducing a phosphatase that inhibits T-cell receptor downstream signaling (2, 4, 5). In addition, effects on other lymphocyte subsets have been described, including an enhancement of regulatory T cell (Treg) proliferation and suppressive activity (6), and a decrease in the activity of both B cells and natural killer (NK) cells (7).

Therapeutic blockade of PD-1 or PD-L1 with monoclonal antibodies leads to durable tumor regressions in patients with several cancer types (8–12). These emerging clinical data have led to the approval by the FDA of two antibodies to PD-1 for the treatment of metastatic melanoma and lung cancer, the humanized IgG4 antibody pembrolizumab (MK-3475) and nivolumab (BMS-936558).

Clinical responses to PD-1 blockade are associated with increased PD-L1 expression on tumor-resident cells, induced by preexisting tumor-infiltrating lymphocytes (TIL), in what is termed "adaptive immune resistance" (1, 10, 13). Patient biopsies obtained from patients before and on therapy with pembrolizumab showed that intratumoral $CD8^+$ T cells proliferated only in patients with an objective response to therapy, as assessed by quantitative immunohistochemistry (IHC). However, it is currently unclear which T-cell functional subsets are involved in this response, and other tumor microenvironment hematopoietic lineage cells have not been well characterized in patient samples.

In the current study, we undertook a comprehensive analysis using multicolor flow cytometry and single-cell multiparametric data interpretation of immune cell infiltrates, particularly in T cells, in biopsies of patients with metastatic melanoma treated with PD-1 blockade.

[1]Division of Hematology-Oncology, Department of Medicine, University of California Los Angeles, Los Angeles, California. [2]Division of Surgical-Oncology, Department of Surgery, University of California Los Angeles, Los Angeles, California. [3]Department of Molecular and Medical Pharmacology, University of California Los Angeles, Los Angeles, California. [4]Jonsson Comprehensive Cancer Center, Los Angeles, California. [5]Center for Biological Sequence Analysis, Department of Systems Biology, Technical University of Denmark, Lyngby, Denmark. [6]Departments of Biological Sciences and Systems Biology, Columbia University, New York, New York. [7]CytoAnalysis, Denver, Colorado. [8]Department of General Internal Medicine and Healthy Services Research, University of California Los Angeles, Los Angeles, California. [9]Department of Medicine, Division of Dermatology. University of California Los Angeles, Los Angeles, California. [10]Center for Immunotherapy, Roswell Park Cancer Institute, Buffalo, New York.

Note: Supplementary data for this article are available at Cancer Immunology Research Online (http://cancerimmunolres.aacrjournals.org/).

Corresponding Authors: Begoña Comin-Anduix, University of California Los Angeles, room 54-140 CHS, 10833 Le Conte Avenue, Los Angeles, CA 90095-1782. Phone: 310-267-2211; Fax: 310-825-4437; E-mail: bcomin@mednet.ucla.edu; or Antoni Ribas, Department of Medicine, Division of Hematology-Oncology, Jonsson Comprehensive Cancer Center (JCCC) at the University of California Los Angeles (UCLA), 11-934 Factor Building; 10833 Le Conte Avenue, Los Angeles, CA 90095-1782. Phone: 310-206-3928; E-mail: aribas@mednet.ucla.edu

doi: 10.1158/2326-6066.CIR-15-0210

Published OnlineFirst January 19, 2016; DOI: 10.1158/2326-6066.CIR-15-0210

Materials and Methods

Clinical trial and study samples

We collected baseline and at least one tumor biopsy while patients were on treatment with pembrolizumab, taken at a mean time of 74 days (range, 15 to 230 days) from 53 patients with metastatic melanoma (stage M1a to M1c; Table 1) treated with pembrolizumab within a phase I clinical trial at UCLA (UCLA IRB 11-003066; NCT01295827) between January of 2012 and May 2013. Patients received single-agent pembrolizumab intravenously at one of three dosing regimens, 0 mg/kg every 2 weeks, or 2 mg/kg or 10 mg/kg every 3 weeks. Three patients had two baseline biopsies, and one patient had three baseline biopsies in different metastatic lesions, for a total of 62 baseline biopsies. Tumor response was assessed at 3 months, with scans performed at 3-month intervals thereafter.

Isolation of single-cell leukocytes from biopsies and peripheral blood

Pieces of tumors from dermatologic, surgical, or image-guided biopsies were mechanically dissociated, centrifuged at 500 g for 5 minutes, and the pellets collected. Cells were either stained immediately or, in a few cases, cryopreserved as described (14). Peripheral blood mononuclear cells (PBMC) were isolated as described in Ibarrondo and colleagues (14).

Flow cytometry surface staining

TILs and PBMCs were stained and acquired in an LSR II Flow Cytometer (BD Biosciences) as described by Ibarrondo and colleagues (14). A description of flow antibody reagents used is on Supplementary Table S1. Panel 1 in that table defines white blood cell (WBC) subpopulations, such as B cells, NK cells, T cells, Tregs, monocytic myeloid-derived suppressor cells (moMDSC), and monocytes. Panel 2 characterizes different T-cell subsets. Panels 3 and 4 designate putative memory T stem cells (T_{MSC}; refs. 15, 16). A healthy donor sample of PBMCs (IRB# 10-001598) or PBMCs from patients was stained and run in parallel with the TIL sample as an internal quality control for staining and gating strategies. Of note, although we analyzed the PD-1 marker by flow cytometry (clone MIH4; Affimetrix), it was discarded from the final analysis after noting that MIH4 and pembrolizumab cross-reacted on the same binding site.

Flow cytometry analysis

All flow data analyses were done with either FlowJo (Tree Star Inc.) or cyt software for visualizing viSNE maps (17). The gating strategy is described in Supplementary Figs. S1 to S3. Biexponential display was used in the analyses. The CytoAnalytics program Vasco (version 1.1.3) is based on exhaustive expansion software (18). One of its functions allows the analysis of all of the possible combinations (positive, negative, and unspecified) from the results of the FlowJo analysis. The statistical parameters of the filter utilized were a delta minimum of 2 and baseline readout ≥ 1, baseline versus treated, or responder versus nonresponders P value of ≤ 0.05, excluding null P values. Delta was defined as day of treatment minus baseline, and it serves to prevent large fold changes when the baseline is small (18). We also used the viSNE software program (17), where we gated for live lymphocytes and then removed all of the events found to be negative for all phenotypical markers. Then we used the viSNE algorithm with the cyt software package on the remaining cells.

Table 1. Patient characteristics

	Total patients, 53; mean age, 65	
	Responders	**Nonresponders**
Number of patients (M/F)	19 (16/3)	34 (24/10)
Mean age (M/F)	68 (69/65)	54 (66/58)
Stage		
M0	0	0
M1a	3	4
M1b	8	7
M1c	8	23
Brain metastasis		
Yes	5	4
No	14	30
LDH		
Normal	17	18
Elevated	2	16
BRAF status		
Wild type	14	22
V600E positive	3	8
V600E heterozygous	1	0
K601E positive	0	1
Others (NRAS mutated + monosomy 3)	1	3
Prior treatment		
None	4	3
Radiation only (R)	1	4
Chemotherapy only (C)	0	0
Immunotherapy only (I)	4	10
BCG	1	0
IFN (interferon)	0	2
Ipilimumab	2	2
Ipilimumab + IFN	0	1
Ipilimumab + IL2	0	5
Targeted therapy only (T)	0	0
Adoptive cell therapy (A)	2	0
Combined treatment	10	17
I + C	1	4
I + R	5	4
I + T	0	1
R + C	0	1
I + R + C	0	1
I + T + A	1	0
I + R + T	2	3
I + T + C	0	1
I + C + T + R	0	2
I + C + T + R + A	1	0
Toxicities (adverse effects)		
Fatigue (grades 1–2)	2	2
Colitis (grades 1–3)	2	1
Pneumonitis (grades 1–2)	1	1
Myalgia (grades 1–2)	0	1
Vitiligo	3	1
Diverticulitis (grades 1–2)	1	0
Liver function test abnormality, grade 3	0	1
Acute kidney injury, grade 4	1	0
Dose of PD-1 antibody		
2 mg/kg	4	14
10 mg/kg	15	18
Response		
Partial response (PR)	12	—
Stable disease (SD)	3	1
Complete response (CR)	4	—
Partial response followed by progression	—	1
Progression of disease (PD)	—	32
Reason for study discontinuation		
Adverse events	2	—
PD	—	31
CR	1	—
Investigator decision	1	—

Abbreviations: BCG, Bacillus Calmette-Guerin; LDH, lactate dehydrogenase.

Published OnlineFirst January 19, 2016; DOI: 10.1158/2326-6066.CIR-15-0210

Statistical analysis

Descriptive statistical analyses were done with GraphPad Prism (GraphPad) and/or the Vasco software program. The Pearson χ^2 test was used for testing difference in the percentage of responders in two dosage groups. Mann–Whitney (unpaired samples) and Wilcoxon matched-pairs signed rank (paired samples) tests were used to compare the pretreatment and on-treatment effect, and/or the Vasco software program. Confidence intervals (CI) were calculated by the Clopper–Pearson method.

Results

Patient demographics and treatment

Fifty-three patients receiving pembrolizumab underwent biopsies for intratumoral cell analyses from February 2012 to May 2013. Table 1 displays the patient characteristics, treatment administered, and clinical outcome. Seven patients (13%) had stage M1a, 15 (28%) had stage M1b, and 31 (58%) had stage M1c metastatic melanoma. Fourteen patients (26%) had prior immunotherapy only, 27 (51%) had previously received other treatments, and seven (13%) were treatment naïve. There was no correlation between the two different doses of pembrolizumab and patient response ($P = 0.18$). One patient was treated under Keynote 002, and his/her dose still remains blinded. Three (4%) patients had grade 3 or 4 toxicities on pembrolizumab (one with grade 3 elevation of liver function test, one with grade 3 colitis, and the other with grade 4 acute kidney injury). The rest of the toxicities were grade 1 or 2 in 14 (28%) patients, including vitiligo, myalgia, diverticulitis, fatigue, colitis, and pneumoniti. Nineteen (36%) patients had an objective tumor response, whereas 34 (64%) were nonresponders by the RECIST 1.1 criteria (19).

Intratumoral T-cell, B-cell, and moMDSC frequency on PD-1 blockade

Twenty-seven baseline and 24 on-therapy tumor biopsies were analyzed to study changes in TILs (WBC) subsets (Supplementary Fig. S1). The percentage of cells expressing leukocyte common antigen ($CD45^+$) in tumor biopsies increased, independent of clinical response, on PD-1 blockade (Fig. 1A). Of these $CD45^+$ cells, the percentage of T cells ($CD3^+$; $P = 0.01$) and B cells ($CD19^+CD3^-$ and $CD20^+CD3^-$; $P = 0.04$) increased in biopsies taken on treatment. Tumors from responding patients on therapy

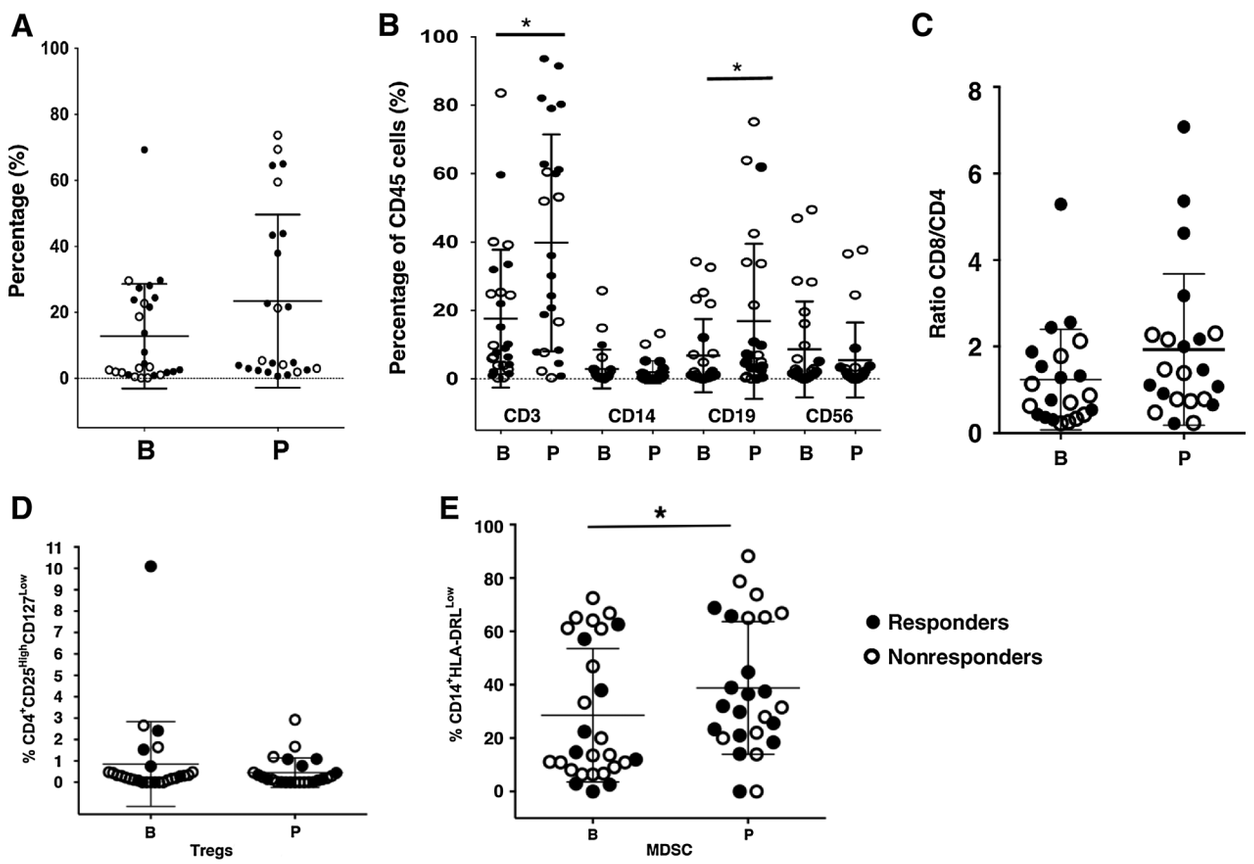

Figure 1.

Changes in leukocyte subpopulations on PD-1 blockade therapy in tumor samples. A, frequency of leukocytes ($CD45^+$) before (B, $n = 27$) and on ($n = 24$) anti–PD-1 therapy. B, among leukocytes, percentage of T cells ($CD3^+$; *, $P = 0.02$), monocytes ($CD14^+$; $P = 0.476$), NK cells ($CD56^+$; $P = 0.47$), and B cells ($CD19/20^+$; *, $P = 0.04$; $n = 29$, before therapy; $n = 25$, on therapy). C, proportion of the ratio for CD8/CD4 cells in paired samples ($n = 22$ pairs; $P = 0.0542$; Wilcoxon test). D, changes in the percentage of Treg ($n = 42$, before; $n = 35$, on therapy; $P = 0.54$). E, changes in the percentage of moMDSC ($n = 27$, before; $n = 25$, on therapy; *, $P = 0.04$). Mean ±SD are provided. Solid circles represent responders; open circles represent nonresponders. B, before treatment; *n*, number of biopsies analyzed; and P, on anti–PD-1 therapy.

Published OnlineFirst January 19, 2016; DOI: 10.1158/2326-6066.CIR-15-0210

contained a higher percentage of T cells. The percentage of monocytes ($CD14^+$) and $CD56^+CD3^-$ NK cells showed no significant change on treatment (Fig. 1B). Among T cells, there was a nonsignificant increase in the ratio of $CD8^+/CD4^+$ T cells when examining 22 pairs of tumors pretreatment and on treatment ($P = 0.054$; Fig. 1C). The frequency of the late activation marker HLA-DR, but not the CD25 early activation marker (refs. 20, 21; gating strategy described in Supplementary Fig. S2A and S2C), was slightly increased in both $CD4^+$ and CD8 ($CD4^-$) T-cell subsets ($CD4^+$: $P = 0.024$; $CD4^-$: $P > 0.05$; Supplementary Fig. S2B). A marginal increase was evident in B cells expressing the activation marker HLA-DR in tumors from patients who were treated (Supplementary Fig. S2D).

Two types of immune-suppressor cells were studied. Tregs were defined by the phenotype of $CD45^+CD3^+CD4^+CD25^{High}CD127^{Low}$ (22); the proportion of Tregs changed little on treatment (Fig. 1D). In addition, we assessed the percentage of moMDSC, based on the phenotype of $CD45^+CD14^+HLA\text{-}DR^{Low}$ (refs. 23–25; Supplementary Fig. S1), and found them significantly increased on treatment ($P = 0.04$; Fig. 1E). No differences between responders and nonresponders were detected for either population of immune-suppressor cells within the TILs, at baseline or while on PD-1 blockade.

Baseline T-cell infiltrates

To analyze the status of T cells at baseline, we assessed the $CD3^+$ T-cell population for relevant immune phenotype markers (Fig. 2). Most T cells had a phenotype of previous exposure to cognate antigen, revealed by expression of CD45RO. Some T cells had a naïve phenotype expressing CD45RA, IL7 receptor α (CD127), and CD62L, but few cells expressed CCR7. The costimulatory marker CD28 was expressed more frequently than CD27. We also analyzed three markers (CD95, CD57, and PD-1) that are usually expressed by effector T cells, terminally differentiated T cells, or exhausted T cells (26); we observed a high expression of CD95, but lower CD57 and PD-1 at baseline.

Tumor-infiltrating $CD45RO^+CD8^+$ T cells increased on anti–PD-1 therapy

In order to further characterize T-cell subsets, we analyzed the 14-parameter flow cytometry data (Supplementary Fig. S3), using multiparametric single-cell resolution in 46 baseline and 37 on-treatment biopsies. Of the 19,683 possible phenotypes analyzed, we discarded all phenotypes with either P values higher than 0.05 and less than 0.05, but with upper or lower 95% CI close to zero. We found a significant increase in the

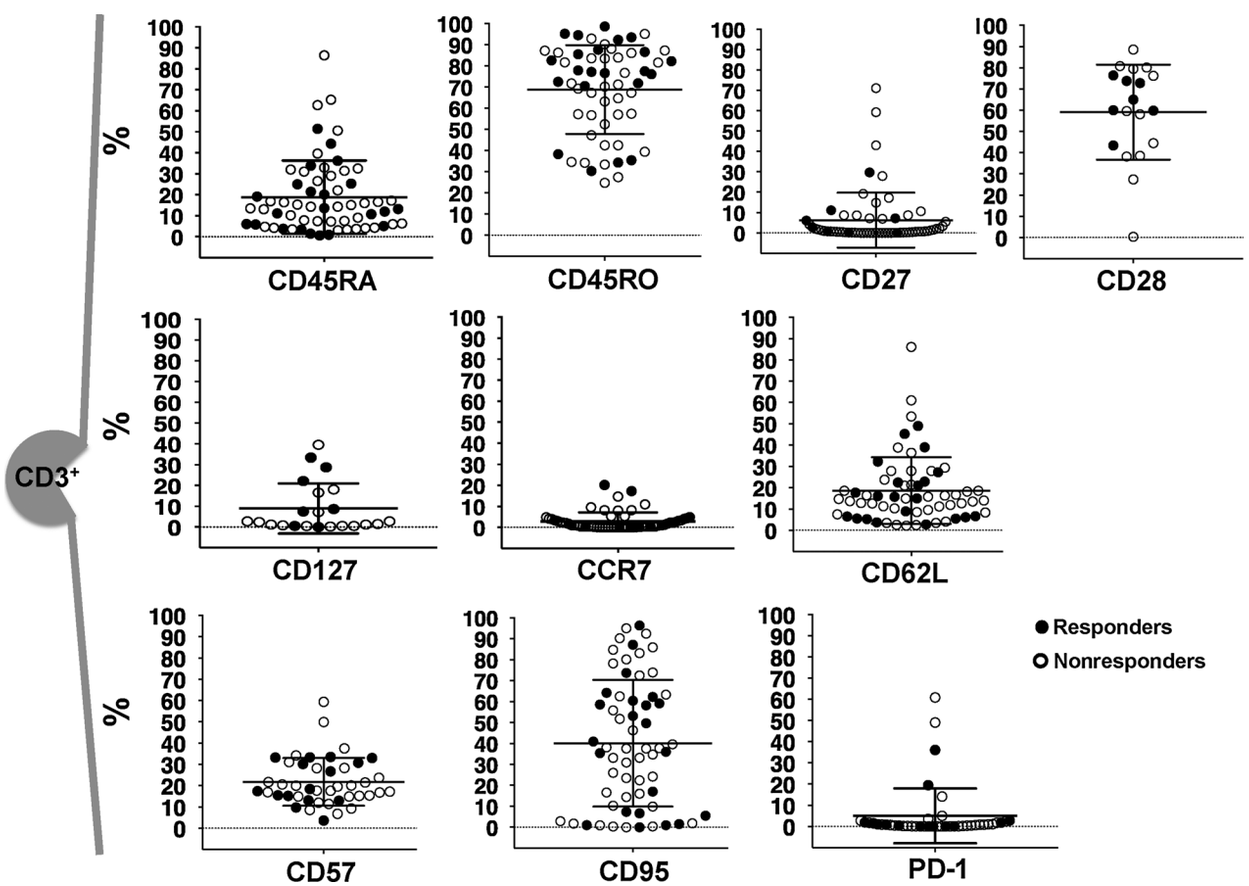

Figure 2.
Phenotype analysis of T cells from baseline tumors. The following $CD3^+$ T-cell markers were plotted prior to any treatment. In order: CD45RA, $n = 62$; CD45RO, $n = 58$; CD27, $n = 62$; CD28, $n = 19$; CD127, $n = 19$; CCR7, $n = 62$; CD62L; $n = 62$; CD57, $n = 43$; CD95, $n = 62$; and PD-1, $n = 44$. All the markers are expressed in percentages. Mean ± SD are provided. n = number of biopsies analyzed. Solid circles represent responders; open circles represent nonresponders.

Published OnlineFirst January 19, 2016; DOI: 10.1158/2326-6066.CIR-15-0210

frequency of $CD8^+$ T cells expressing the memory marker CD45RO in combination with the absence of CD57, CCR7, and CD27, which corresponds to an effector memory T-cell (T_{EM}) phenotype (Fig. 3A) in biopsies obtained while on anti–PD-1. Figure 3B and C show the phenotype with the least number of immune markers ($CD8^+CD4^-CD45RO^+$), the phenotype with the highest number of immune markers ($CD8^+CD4^-CD45RO^+CCR7^-CD27^-CD57^-$), and T_{EM} phenotypes comparing baseline and on-therapy biopsies. Biopsies from patients who responded had an enrichment of memory T cells on treatment (Fig. 3B and C, right graph; $P = 0.002$ for $CD8^+CD4^-CD45RO^+$; $P = 0.006$ for $CD8^+CD45RO^+CCCR7^-CD27^-CD57^-$). Expression of other phenotypes did not change over time or was lower than 1%. These data demonstrate that $CD8^+$ T_{EM} is the main characterized functional phenotype present in biopsies from patients on anti–PD-1 therapy, in particular in tumors of patients who responded to therapy.

Frequency of tumor-infiltrating $CD45RO^+CD4^+$ T cells on anti–PD-1 therapy

Within the $CD4^+$ T-cell subset ($CD3^+CD8^-CD4^+$), we found a dominant population of $CD4^+$ T cells expressing the memory marker CD45RO that were CD57 negative, in combination with the absence of CCR7, CD62L, and CD45RA (Fig. 4A). The $CD4^+$ T_{EM} phenotypes significantly decreased on anti–PD-1 therapy. On the contrary, the $CD4^+$ effector T-cell–like phenotypes $CD8^-CD4^+CD45RO^+CD57^+$ ($P = 0.047$), and two variations of this phenotype, $CD8^-CD4^+CD45RO^+CCR7^-CD57^+$ ($P = 0.03$) and $CD8^-CD4^+CD45RO^+CCR7^-CD62L^-CD57^+$ ($P = 0.05$), significantly increased on therapy (Fig. 4B, left graph). Tumors from nonresponding patients had greater percentages of the following phenotypes: $CD8^-CD4^+CD45RO^+CD57^+$ ($P = 0.024$); $CD8^-CD4^+CD45RO^+CCR7^-CD57^+$ ($P = 0.022$); and $CD8^-CD4^+CD45RO^+CCR7^-CD62L^-CD57^+$ ($P > 0.05$; Fig. 4B, right plots; refs. 27, 28). Taken together, these results show a decrease in the percentage of $CD4^+$ T_{EM} in tumors on

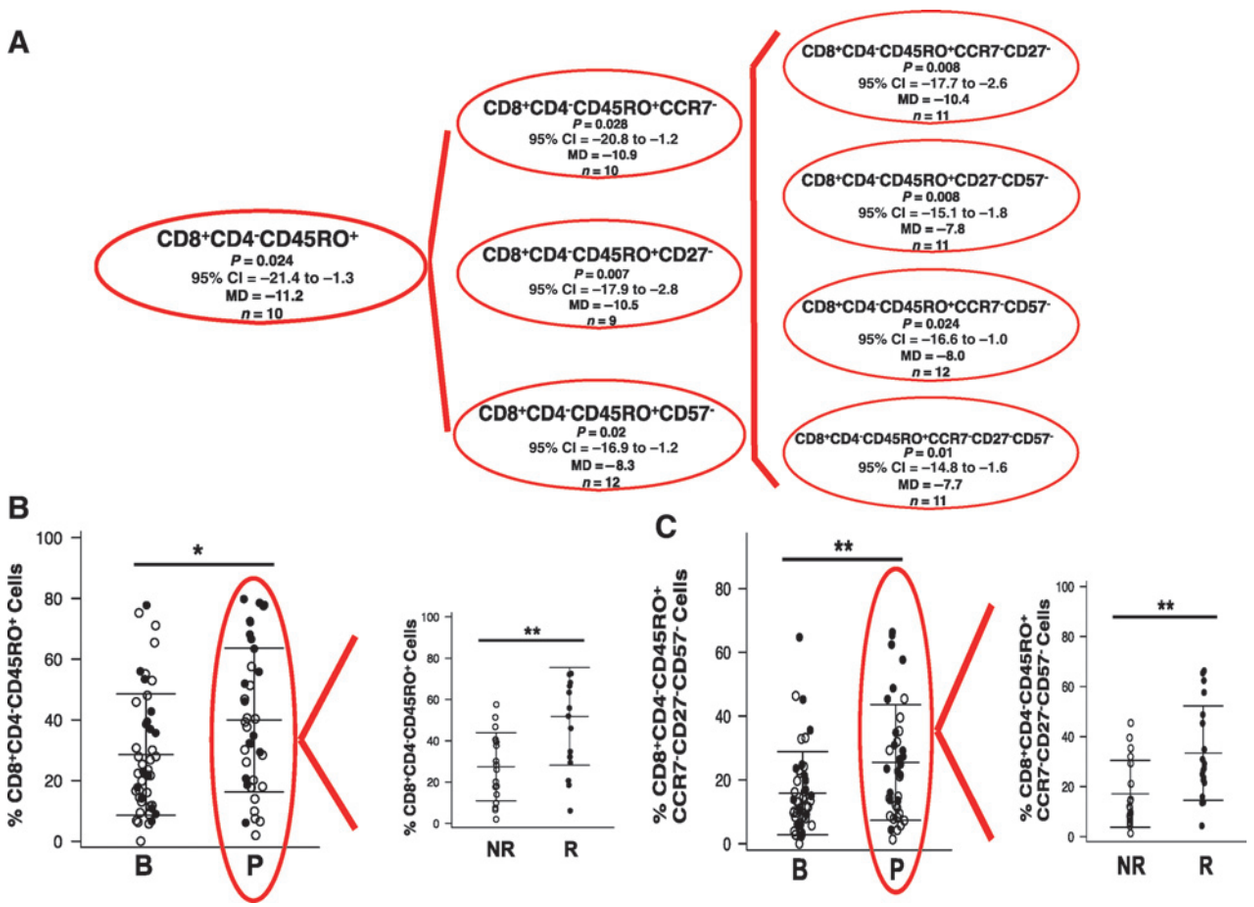

Figure 3.
$CD8^+$ T-cell subsets with significant differences in biopsies on PD-1 blockade therapy. A, dendogram illustrating the frequency of $CD8^+$ T-cell subsets that present lower *P* value ($P \leq 0.05$) with higher 95% confidence interval (95% CI) using CytoAnalysis program. The program presented an increase of the mean difference (MD) and the 95% CI of the baseline and postdose samples as a negative value. *n* describes how many patients of the 18 paired TILs present with that particular phenotype. B, analysis of the percentage of $CD8^+CD4^-CD45RO^+$ phenotype (*, $P = 0.02$), displaying a higher percentage of the responders (**, $P = 0.002$). C, analysis of the percentage of the more extended combination of phenotype markers $CD8^+CD4^-CD45RO^+CCR7^-CD27^-CD57^-$ (**, $P = 0.01$), being augmented in responding patients (**, $P = 0.006$, right plot). The ongoing treatment (red circle) was arranged by responder and nonresponder tumors (right plot). Mean ± SD are provided. B, before treatment; *n*, number of biopsies; P, on anti–PD-1 therapy.

Published OnlineFirst January 19, 2016; DOI: 10.1158/2326-6066.CIR-15-0210

pembrolizumab treatment in both responders and nonresponders, and an augmented percentage of $CD4^+$ effector T cells on anti–PD-1 treatment only in tumors of nonresponding patients.

Visualization of changes in $CD8^+$ $CD45RO^+$ T cells in paired biopsies

We then focused the analysis on the nine paired biopsies obtained from patients who responded to therapy. The analysis of changes in $CD8^+CD45RO^+$ T cells was suggestive of a T-memory phenotype (Fig. 5A). The starting lesions were of different sizes, and the postdose tumors were obtained at different time points on-therapy (range, 19 to 186 days; median, 39 days). Five of the biopsies showed an apparent increase in the percentage of $CD8^+CD45RO^+$ cells, whereas three showed a clear decrease. Only one of those patients (patient #47) had both biopsies (before treatment and during treatment) performed from the same lesion, a left suprarenal metastasis. We applied viSNE analysis to better visualize the changes in T cells in this biopsy (Fig. 5B), which provided a global view of all cell subsets simultaneously. This analysis allowed us to conclude that the decrease in the frequency of CD45RO observed in Fig. 5A could be explained by a strong decrease in the total number of T cells in the postdose tumor as observed in Fig. 5B (lower row), likely due to taking the biopsy from a residual regressed tumor.

Analysis of naïve T cells and T_{MSC} cells

We also explored the presence and potential of on-treatment changes in the frequency of naïve-like T-cell (29) and T_{MSC} phenotypes described originally by Gattinoni and colleagues (29) and modified by Cieri and colleagues (16). Both of these populations were present at very low frequencies among TILs at baseline and did not change with treatment (Supplementary Fig. S4).

Changes in WBC subpopulations in peripheral blood

We performed similar analyses in peripheral blood samples from nine baseline and 14 on-therapy blood draws. The percentage of leukocytes slightly decreased on anti–PD-1 treatment, mainly due to a decrease in $CD3^+$ T cells. Monocytes, B cells, and NK cells did not change. The ratio of CD8/CD4 increased slightly (Fig. 6A). We did not observe any change in cells with the Treg or moMDSC (Fig. 6B). There was no statistically significant change in any particular T-cell phenotype comparing baseline and on-therapy blood draws (Fig. 6C).

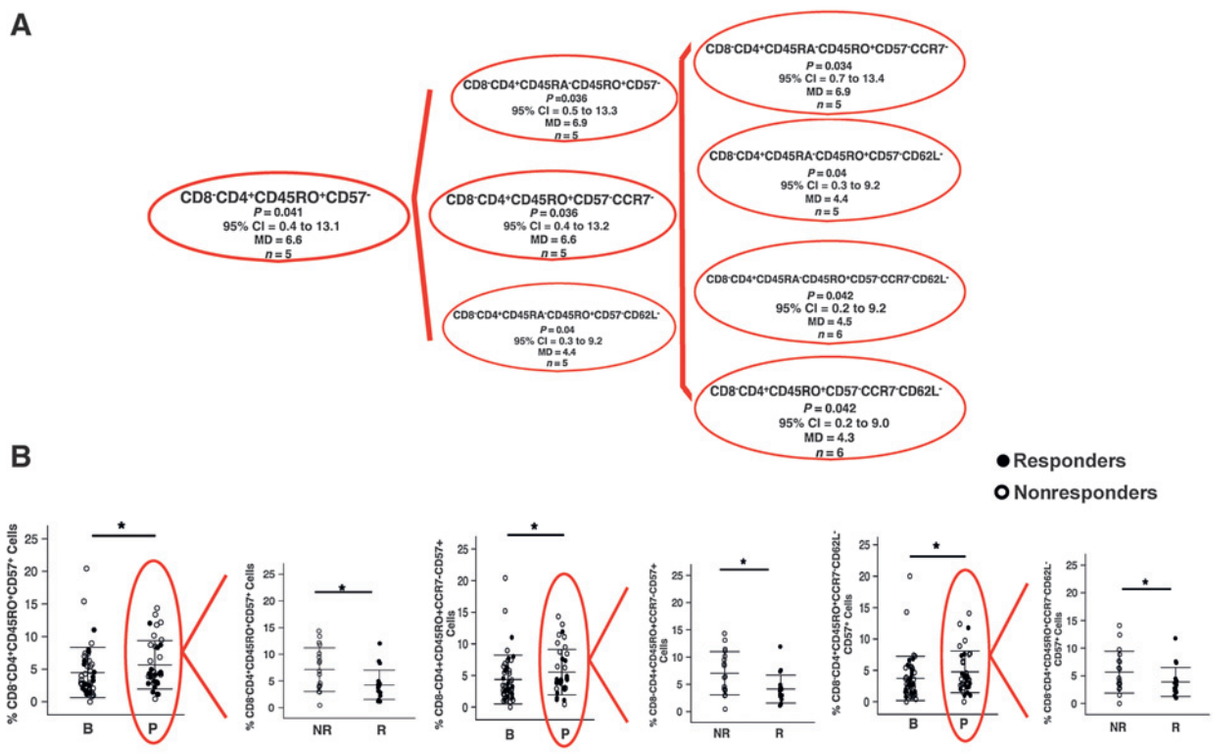

Figure 4.
$CD4^+$ T-cell subsets with statistically significant differences in biopsies on PD-1 blockade therapy. A, dendogram illustrating all $CD4^+$ T cells that present with a lower *P* value ($P \leq 0.05$) with higher 95% CI using CytoAnalysis program. The program presents as positive values a decrease of the mean difference (MD) and the 95% CI of the baseline and postdose samples as a positive value. *n* describes how many patients of the 18 paired TILs show that particular phenotype. B, the percentage of a phenotype of $CD8^-CD4^+CD45RO^+CD57^+$ effector T cells (*, $P = 0.05$) plus two related more extended phenotypes, $CD8^-CD4^+CD45RO^+CCR7^-CD57^+$ (*, $P = 0.003$) and $CD8^-CD4^+CD45RO^+CCR7^-CD62L^-CD57^+$ (*, $P = 0.05$). The ongoing treatment (red circles) was compared between responder and nonresponder tumors (right plot), being the *P* value: $CD8^-CD4^+CD45RO^+CD57^+$: *, $P = 0.024$; $CD8^-CD4^+CD45RO^+CCR7^-CD57^+$: *, $P = 0.022$; and $CD8^-CD4^+CD45RO^+CCR7^-CD62L^-CD57^+$ ($P > 0.05$). B, before treatment; P, on anti–PD-1 therapy. Mean ± SD are provided. Solid circles represent responders; open circles represent nonresponders ($n = 46$ baseline; $n = 37$ treated). B, before treatment; N, nonresponders; P, on anti–PD-1 therapy; R, responders.

Published OnlineFirst January 19, 2016; DOI: 10.1158/2326-6066.CIR-15-0210

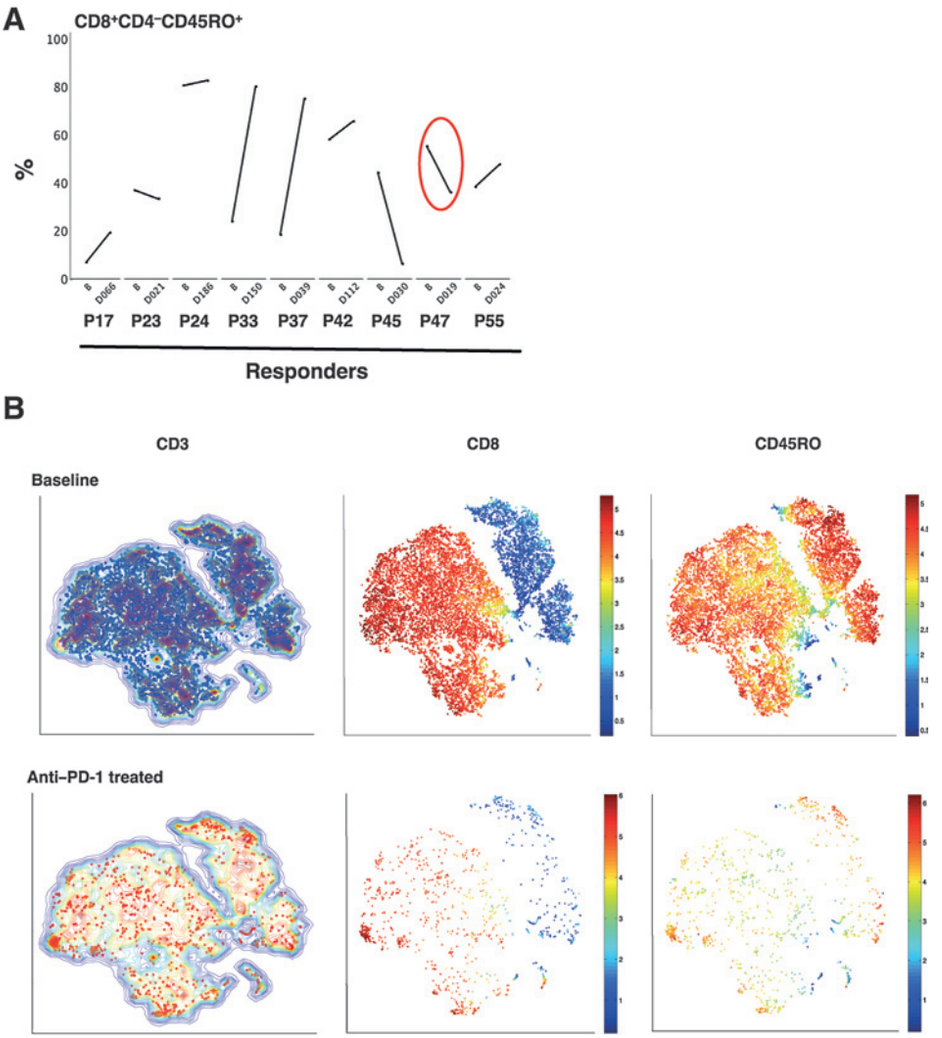

Figure 5.
Comparison of $CD8^+$ memory T-cell phenotypes in paired biopsies from patients with a response to anti–PD-1 therapy. A, paired longitudinal analysis of the frequency of $CD8^+$ $CD4^-CD45RO^+$ at baseline and on anti–PD-1 treatment by exhaustive expansion software. B, baseline; DXXX, day of blood draw from start of anti–PD-1 treatment; PXX, patient identifier; $n = 9$ patients. B, visualization of the CD45RO T cells from the suprarenal biopsy from patient #47 19 days on therapy. Contour plots of the viSNE maps gated on $CD3^+$ and $7AAD^-CD16^-$ $CD19^-$ (live cells). The contour plots show cell density in each region of the map. Each dot in the viSNE map depicts the location of an individual cell, and its color represents the expression of its immune cell marker. $CD3^+$ T-cell (left column) contour plots before (blue) and on anti–PD-1 blockade therapy (red). The expression of $CD8^+$ T cells (in red) and $CD4^+$ T cells (in blue) cells inside the CD3 T-cell contour plot is shown in the middle column. In the right column, CD45RO (in red) is shown. Red color indicates high, orange indicates medium, and blue represents low expression of the marker on the cell surface.

To better analyze any potential changes in leukocyte populations upon PD-1 blockade that were not evident by the combinatorial gating analysis, we applied the viSNE program. viSNE is not limited to high-low thresholds and can discern mid-level phenotypes, as well as nonlinear relations between markers, and hence is capable of searching for more complex phenotypes. We mapped the T cells of two responders and nonresponders facilitating a comprehensive comparison of all the cell phenotypes (Fig. 6D and E). Responders were patients #4 and #45, with blood taken at 59 and 41 days from study start, respectively. Nonresponders were patients #12 and #14 with the blood collected 42 and 60 days from study start, respectively. A distinct population of leukocytes had high expression of HLA-DR and CD56, and mid-level expression of CD14 and CD4. This population of cells increased by 9-fold in both on-treatment peripheral blood samples from the patients with a response to therapy.

Discussion

In this study, we performed a thorough characterization of TILs in tumors from patients treated with PD-1 blockade therapy. The major finding was the increase in the frequency of memory T cells in patients with a tumor response, where the principal immune marker was $CD8^+CD4^-CD45RO^+$ and combinations of it, giving a final most common phenotype of T_{EM} cells. This finding is consistent with the anticipated mechanism of action of this therapy. However, we would anticipate an increase in the frequency of $CD8^+$ T cells with an effector phenotype, which we were not able to document. As opposed to the changes in $CD8^+$ T cells, we did find $CD4^+$ T cells expressing CD57, an effector T-cell phenotype also called proliferation-incompetent CD4 T cells, as they have been reported to produce IFNγ but have limited proliferation capacity (30). $CD4^+CD57^+$ T cells increased in tumors from patients with disease progression as opposed to responding lesions. Tumor-infiltrating T_{EM} cells have been found in other studies and may have good prognostic implications. Pagès and colleagues reported a T_{EM} phenotype in primary tumors of patients with colorectal cancer analyzed by flow cytometry (31). Furthermore, Koelzer and colleagues reported the presence of CD8 and CD45RO-positive TILs, which correlated with improved survival in patients, based on the IHC analysis of colorectal carcinoma samples (32).

Published OnlineFirst January 19, 2016; DOI: 10.1158/2326-6066.CIR-15-0210

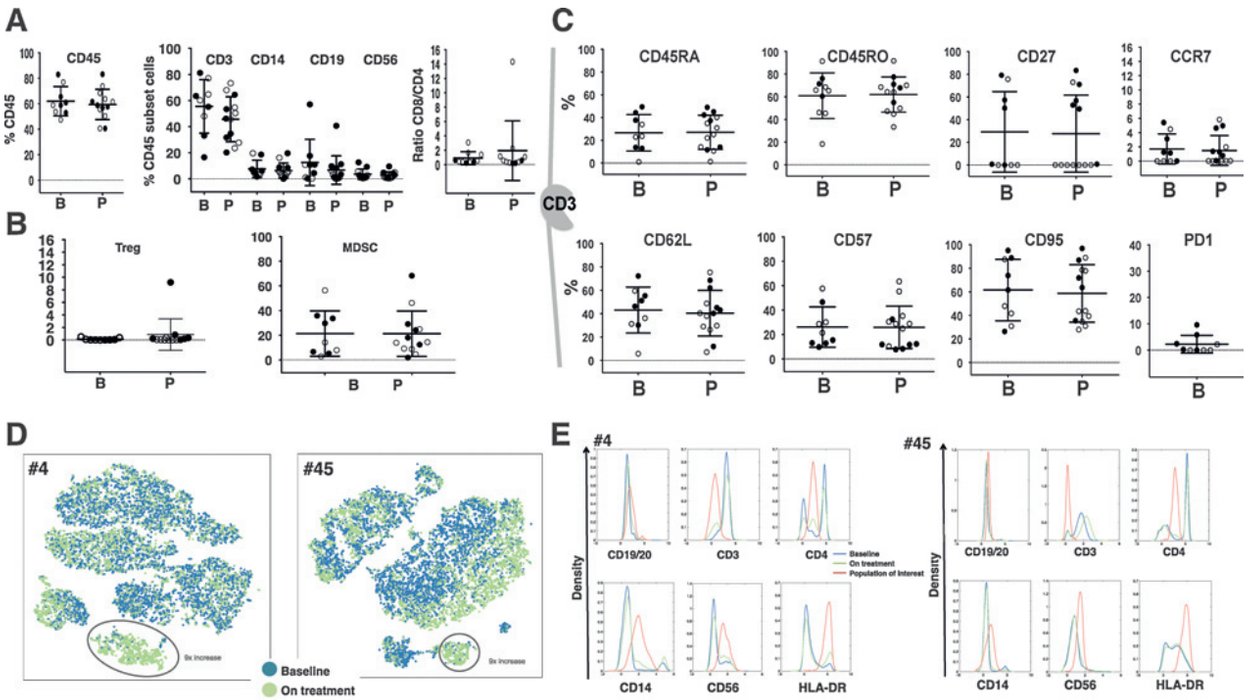

Figure 6.

Analysis of peripheral blood samples at baseline and on anti–PD-1 therapy. A, dot plots depicting the percentage of leukocytes ($CD45^+$) on the left, the percentage of T ($CD3^+$), monocytes ($CD14^+$), B cells ($CD19^+/CD20^+$), and NK cells ($CD56^+$) in the center, and the ratio of CD8/CD4 on the right (B, $n = 9$; P, $n = 13$). B, dot plots of suppressor cells. Tregs are on the left, and moMDSC on the right. C, dot plots of the T-cell subset, CD45RA, CD45RO, CD27, CCR7, CD62L, CD57, CD95 (B, $n = 9$; P, $n = 14$), and PD-1 only at baseline ($n = 9$). Mean ± SD are provided. B, before treatment; P, on anti–PD-1 therapy; *n*, number of biopsies analyzed. Solid circles represent responders; open circles represent nonresponders. D and E, viSNE analysis from blood from 2 patients who responded to anti–PD-1 (patients #4 and #45) identified differences between the baseline and on-treatment samples. D, the viSNE map of the baseline (blue) and on-treatment (green) sample showed the presence of a distinct population (events within the circle). E, histogram representation of the population of interest (red) identified from the viSNE plot at baseline (blue) and on treatment (green). The CD19, CD56, CD14, CD3, CD4, CD127, CD25, and HLA-DR channels of the baseline and on-treatment samples were chosen for analysis by viSNE. The marker expression is shown on the *x*-axis, and the density of cells is shown on the *y*-axis.

Our findings of an enhanced proportion of cells with a phenotype of moMDSC (24) in patients' on-therapy biopsies from both responders and nonresponders could be interpreted as a by-product of inflammation in the tumor microenvironment on PD-1 blockade (33, 34). In fact, IHC and transcriptome analyses of on-therapy tumor biopsies suggest that several inflammatory cells and markers increase with anti–PD-1 or anti–PD-L1 treatment (10, 13). The same process may attract B cells into tumors obtained from patients on treatment. The significant enrichment of B cells in the tumor microenvironment may have a role in local antigen presentation (35). However, we could not link these B cells to tertiary lymphoid structures (36, 37) as our approach, based on single-cell flow cytometry analysis of tumor lysates, does not preserve tissue morphology (38) as does IHC (39).

Polychromatic flow cytometry has flourished over the past decade (40, 41), and it has been one of the primary factors contributing to the ability to document the heterogeneity of immune cells at the single-cell level (42). However, until recently, the ability to plot multidimensional flow data has remained a challenge despite efforts to simplify it with different computational methods (17,43–45). We chose to work with the Vasco (18) and the viSNE programs (17). The former has the advantage of the simplicity of the plots, the flexibility of the filters used to scan results across the sets, and the ability to study the weight of each immune marker from one at a time to all simultaneously (18). The latter has the ability to visualize the multidimensional data in simple two-dimensional plots maintaining the nonlinearity and geometry of the sample at the single-cell level. Thus, the strengths of the approach are the visualization of the samples and the simultaneous integration of all of the dimensions (17). In our studies, the application of both programs provided complementary data and improved our understanding of the immune cells in biopsies from patients treated with anti–PD-1.

The effects of PD-1 blockade in cells circulating in peripheral blood were minimal compared with the changes in tumors. No major characterized blood cell subtype changed significantly. However, a population of cells with both monocyte and T-cell markers was detected in on-treatment blood samples from 2 of 4 patients. Monocytes expressing CD56 have been previously described in peripheral blood by Gruenbacher and colleagues (46). Moreover, we cannot rule out the possibility that these cells may be the human counterpart of the mice iKDC or premature NK cells. In a study of patients with refractory gastrointestinal stromal tumors, $HLA\text{-}DR^+CD56^+$ cells correlated with overall survival and progression-free survival after treatment with imatinib mesylate and IL2 (47).

In conclusion, anti–PD-1 therapy results in an intratumoral increase in the frequency of T cells, B cells, and MDSCs. Memory T-cell phenotypes were found specifically increased in patients whose tumors responded to therapy. In contrast, changes were

Published OnlineFirst January 19, 2016; DOI: 10.1158/2326-6066.CIR-15-0210

minor in peripheral blood cells, although we could detect an unusual population of what may be a subset of dendritic cells or HLA-DR NK cells in some responding patients. Despite being subjected to challenges derived from tumor heterogeneity that can drive different human immune signatures (48, 49), the different anatomical locations of the biopsies, the relatively small sample size, and the different collection time points, we have found some common characteristics in the intratumoral T-cell populations in melanoma biopsies from the responding patients. Our results help advance the knowledge of the effects of PD-1 blockade on the human T cells of the immune system.

Disclosure of Potential Conflicts of Interest

A. Ribas is a consultant/advisory board member for Merck. J. Siebert has ownership interest (including patents) in CytoAnalytics. B. Chmielowski has received honoraria from the speakers bureau of Bristol-Myers Squibb, Genentech, and Prometheus; and is a consultant/advisory board member for Amgen, Astellas, Bristol-Myers Squibb, Genetech, Lilly, and Merck. No potential conflicts of interest were disclosed by the other authors.

Authors' Contributions

Conception and design: A. Ribas, B. Chmielowski, B. Comin-Anduix
Development of methodology: T. Chodon, D. Pe'er, B. Comin-Anduix
Acquisition of data (provided animals, acquired and managed patients, provided facilities, etc.): E. Avramis, C. Kivork, B. Chmielowski, P.C. Tumeh, T. Chodon, B. Comin-Anduix
Analysis and interpretation of data (e.g., statistical analysis, biostatistics, computational analysis): A. Ribas, D.S. Shin, J. Zaretsky, J. Frederiksen, A. Cornish, E. Avramis, J. Siebert, X. Wang, B. Chmielowski, D. Pe'er, B. Comin-Anduix
Writing, review, and/or revision of the manuscript: A. Ribas, D.S. Shin, E. Avramis, P. Kaplan-Lefko, X. Wang, B. Chmielowski, J.A. Glaspy, P.C. Tumeh, T. Chodon, B. Comin-Anduix
Administrative, technical, or material support (i.e., reporting or organizing data, constructing databases): A. Ribas, E. Seja, C. Kivork, P. Kaplan-Lefko, B. Chmielowski, P.C. Tumeh, B. Comin-Anduix
Study supervision: A. Ribas, B. Chmielowski, B. Comin-Anduix

Acknowledgments

Flow cytometry was performed in the UCLA Jonsson Comprehensive Cancer Center (JCCC) and Center for AIDS Research. The authors thank Rongqing Guo and Li Wang for technical support.

Grant Support

A. Ribas has received NIH grants R35 CA197633, P01 CA168585, and Stand Up To Cancer – Cancer Research Institute (SU2C-CRI) Cancer Immunology Dream Team Translational Research Grant (SU2C-AACR-DT1012). A. Ribas and D. Pe'er were supported by a Stand Up To Cancer Phillip A. Sharp Innovation in Collaboration Award (SU2C-AACR-PS04). D.S. Shin was supported by Oncology (5T32CA009297-30), Dermatology (5T32AR058921-05), and Tumor Immunology (5T32CA009120-39) training grants and a Tower Cancer Research Foundation Grant. The Flow Cytometry Core Facility is supported by NIH grants CA16042 and AI 28697, and by the JCCC, the UCLA AIDS Institute, and the David Geffen School of Medicine at UCLA.

The costs of publication of this article were defrayed in part by the payment of page charges. This article must therefore be hereby marked *advertisement* in accordance with 18 U.S.C. Section 1734 solely to indicate this fact.

Received August 26, 2015; revised November 23, 2015; accepted December 4, 2015; published OnlineFirst January 19, 2016.

References

1. Pardoll DM. The blockade of immune checkpoints in cancer immunotherapy. Nat Rev Cancer 2012;12:252–64.
2. Ishida Y, Agata Y, Shibahara K, Honjo T. Induced expression of PD-1, a novel member of the immunoglobulin gene superfamily, upon programmed cell death. EMBO J 1992;11:3887–95.
3. Ahmadzadeh M, Johnson LA, Heemskerk B, Wunderlich JR, Dudley ME, White DE, et al. Tumor antigen-specific CD8 T cells infiltrating the tumor express high levels of PD-1 and are functionally impaired. Blood 2009;114:1537–44.
4. Sheppard KA, Fitz LJ, Lee JM, Benander C, George JA, Wooters J, et al. PD-1 inhibits T-cell receptor induced phosphorylation of the ZAP70/CD3zeta signalosome and downstream signaling to PKCtheta. FEBS Lett 2004;574:37–41.
5. Okazaki T, Maeda A, Nishimura H, Kurosaki T, Honjo T. PD-1 immunoreceptor inhibits B cell receptor-mediated signaling by recruiting src homology 2-domain-containing tyrosine phosphatase 2 to phosphotyrosine. Proc Natl Acad Sci U S A 2001;98:13866–71.
6. Francisco LM, Salinas VH, Brown KE, Vanguri VK, Freeman GJ, Kuchroo VK, et al. PD-L1 regulates the development, maintenance, and function of induced regulatory T cells. J Exp Med 2009;206:3015–29.
7. Terme M, Ullrich E, Aymeric L, Meinhardt K, Desbois M, Delahaye N, et al. IL-18 induces PD-1-dependent immunosuppression in cancer. Cancer Res 2011;71:5393–9.
8. Topalian SL, Sznol M, McDermott DF, Kluger HM, Carvajal RD, Sharfman WH, et al. Survival, durable tumor remission, and long-term safety in patients with advanced melanoma receiving nivolumab. J Clin Oncol 2014;32:1020–30.
9. Hamid O, Robert C, Daud A, Hodi FS, Hwu WJ, Kefford R, et al. Safety and tumor responses with lambrolizumab (anti–PD-1) in melanoma. N Engl J Med 2013;369:134–44.
10. Herbst RS, Soria JC, Kowanetz M, Fine GD, Hamid O, Gordon MS, et al. Predictive correlates of response to the anti–PD-L1 antibody MPDL3280A in cancer patients. Nature 2014;515:563–7.
11. Powles T, Eder JP, Fine GD, Braiteh FS, Loriot Y, Cruz C, et al. MPDL3280A (anti–PD-L1) treatment leads to clinical activity in metastatic bladder cancer. Nature 2014;515:558–62.
12. Ansell SM, Lesokhin AM, Borrello I, Halwani A, Scott EC, Gutierrez M, et al. PD-1 blockade with nivolumab in relapsed or refractory Hodgkin's lymphoma. N Engl J Med 2015;372:311–9.
13. Tumeh PC, Harview CL, Yearley JH, Shintaku IP, Taylor EJ, Robert L, et al. PD-1 blockade induces responses by inhibiting adaptive immune resistance. Nature 2014;515:568–71.
14. Ibarrondo FJ, Yang OO, Chodon T, Avramis E, Lee Y, Sazegar H, et al. Natural killer T cells in advanced melanoma patients treated with tremelimumab. PLoS One 2013;8:e76829.
15. Lugli E, Gattinoni L, Roberto A, Mavilio D, Price DA, Restifo NP, et al. Identification, isolation and in vitro expansion of human and non-human primate T stem cell memory cells. Nat Protoc 2013;8:33–42.
16. Cieri N, Camisa B, Cocchiarella F, Forcato M, Oliveira G, Provasi E, et al. IL-7 and IL-15 instruct the generation of human memory stem T cells from naive precursors. Blood 2013;121:573–84.
17. Amir el AD, Davis KL, Tadmor MD, Simonds EF, Levine JH, Bendall SC, et al. viSNE enables visualization of high dimensional single-cell data and reveals phenotypic heterogeneity of leukemia. Nat Biotechnol 2013;31:545–52.
18. Siebert JC, Wang L, Haley DP, Romer A, Zheng B, Munsil W, et al. Exhaustive expansion: A novel technique for analyzing complex data generated by higher-order polychromatic flow cytometry experiments. J Transl Med 2010;8:106.
19. Eisenhauer EA, Therasse P, Bogaerts J, Schwartz LH, Sargent D, Ford R, et al. New response evaluation criteria in solid tumours: revised RECIST guideline (version 1.1). Eur J Cancer 2009;45:228–47.
20. Heeren AM, Koster BD, Samuels S, Ferns DM, Chondronasiou D, Kenter GG, et al. High and interrelated rates of PD-L1+CD14+ antigen-presenting cells and regulatory T cells mark the microenvironment of metastatic lymph nodes from patients with cervical cancer. Cancer Immunol Res 2015;3:48–58.
21. Chao KH, Wu MY, Yang JH, Chen SU, Yang YS, Ho HN. Expression of the interleukin-2 receptor alpha (CD25) is selectively decreased on decidual CD4+ and CD8+ T lymphocytes in normal pregnancies. Mol Hum Reprod 2002;8:667–73.

22. Seddiki N, Santner-Nanan B, Martinson J, Zaunders J, Sasson S, Landay A, et al. Expression of interleukin (IL)-2 and IL-7 receptors discriminates between human regulatory and activated T cells. J Exp Med 2006;203: 1693–700.
23. Tarhini AA, Butterfield LH, Shuai Y, Gooding WE, Kalinski P, Kirkwood JM. Differing patterns of circulating regulatory T cells and myeloid-derived suppressor cells in metastatic melanoma patients receiving anti-CTLA4 antibody and interferon-alpha or TLR-9 agonist and GM-CSF with peptide vaccination. J Immunother 2012;35:702–10.
24. Filipazzi P, Valenti R, Huber V, Pilla L, Canese P, Iero M, et al. Identification of a new subset of myeloid suppressor cells in peripheral blood of melanoma patients with modulation by a granulocyte-macrophage colony-stimulation factor-based antitumor vaccine. J Clin Oncol 2007;25: 2546–53.
25. Poschke I, Mougiakakos D, Hansson J, Masucci GV, Kiessling R. Immature immunosuppressive CD14+HLA-DR-/low cells in melanoma patients are Stat3hi and overexpress CD80, CD83, and DC-sign. Cancer Res 2010;70:4335–45.
26. Apetoh L, Smyth MJ, Drake C, Abastado J-P, Apte RN, Ayyoub M, et al. Consensus nomenclature for CD8+ T cell phenotypes in cancer. OncoImmunology 2015; 4:e998538.
27. Chattopadhyay PK, Betts MR, Price DA, Gostick E, Horton H, Roederer M, et al. The cytolytic enzymes granyzme A, granzyme B, and perforin: expression patterns, cell distribution, and their relationship to cell maturity and bright CD57 expression. J Leukoc Biol 2009;85:88–97.
28. Gattinoni L, Powell DJ Jr, Rosenberg SA, Restifo NP. Adoptive immunotherapy for cancer: building on success. Nat Rev Immunol 2006;6:383–93.
29. Gattinoni L, Lugli E, Ji Y, Pos Z, Paulos CM, Quigley MF, et al. A human memory T cell subset with stem cell-like properties. Nat Med 2011;17: 1290–7.
30. Palmer BE, Blyveis N, Fontenot AP, Wilson CC. Functional and phenotypic characterization of CD57+CD4+ T cells and their association with HIV-1-induced T cell dysfunction. J Immunol 2005;175:8415–23.
31. Pagès F, Berger A, Camus M, Sanchez-Cabo F, Costes A, Molidor R, et al. Effector memory T cells, early metastasis, and survival in colorectal cancer. N Engl J Med 2005;353:2654–66.
32. Koelzer VH, Lugli A, Dawson H, Hadrich M, Berger MD, Borner M, et al. CD8/CD45RO T-cell infiltration in endoscopic biopsies of colorectal cancer predicts nodal metastasis and survival. J Transl Med 2014;12:81.
33. Ostrand-Rosenberg S, Sinha P. Myeloid-derived suppressor cells: linking inflammation and cancer. J Immunol 2009;182:4499–506.
34. Umansky V, Sevko A, Gebhardt C, Utikal J. Myeloid-derived suppressor cells in malignant melanoma. J Dtsch Dermatol Ges 2014;12:1021–7.
35. Nelson BH. CD20+ B cells: the other tumor-infiltrating lymphocytes. J Immunol 2010;185:4977–82.
36. Carragher DM, Rangel-Moreno J, Randall TD. Ectopic lymphoid tissues and local immunity. Semin Immunol 2008;20:26–42.
37. Drayton DL, Liao S, Mounzer RH, Ruddle NH. Lymphoid organ development: from ontogeny to neogenesis. Nat Immunol 2006;7:344–53.
38. Ruffell B, Au A, Rugo HS, Esserman LJ, Hwang ES, Coussens LM. Leukocyte composition of human breast cancer. Proc Natl Acad Sci U S A 2012;109:2796–801.
39. Fridman WH, Pages F, Sautes-Fridman C, Galon J. The immune contexture in human tumours: impact on clinical outcome. Nat Rev Cancer 2012; 12:298–306.
40. Perfetto SP, Chattopadhyay PK, Roederer M. Seventeen-colour flow cytometry: unravelling the immune system. Nat Rev Immunol 2004;4:648–55.
41. Bendall SC, Nolan GP, Roederer M, Chattopadhyay PK. A deep profiler's guide to cytometry. Trends Immunol 2012;33:323–32.
42. Bendall SC, Nolan GP. From single cells to deep phenotypes in cancer. Nat Biotechnol 2012;30:639–47.
43. Lugli E, Roederer M, Cossarizza A. Data analysis in flow cytometry: the future just started. Cytometry A 2010;77:705–13.
44. Aghaeepour N, Finak G, Flow CAPC, Consortium D, Hoos H, Mosmann TR, et al. Critical assessment of automated flow cytometry data analysis techniques. Nat Methods 2013;10:228–38.
45. Schadt EE, Linderman MD, Sorenson J, Lee L, Nolan GP. Computational solutions to large-scale data management and analysis. Nat Rev Genet 2010;11:647–57.
46. Gruenbacher G, Gander H, Rahm A, Nussbaumer W, Romani N, Thurnher M. CD56+ human blood dendritic cells effectively promote TH1-type gammadelta T-cell responses. Blood 2009;114:4422–31.
47. Chaput N, Flament C, Locher C, Desbois M, Rey A, Rusakiewicz S, et al. Phase I clinical trial combining imatinib mesylate and IL-2: HLA-DR NK cell levels correlate with disease outcome. Oncoimmunology 2013;2: e23080.
48. Jamal-Hanjani M, Quezada SA, Larkin J, Swanton C. Translational implications of tumor heterogeneity. Clin Cancer Res 2015;21:1258–66.
49. Comin-Anduix B, Lee Y, Jalil J, Algazi A, de la Rocha P, Camacho LH, et al. Detailed analysis of immunologic effects of the cytotoxic T lymphocyte-associated antigen 4-blocking monoclonal antibody tremelimumab in peripheral blood of patients with melanoma. J Transl Med 2008;6:22.

Published OnlineFirst January 19, 2016; DOI: 10.1158/2326-6066.CIR-15-0210

AACR American Association for Cancer Research

Cancer Immunology Research

PD-1 Blockade Expands Intratumoral Memory T Cells

Antoni Ribas, Daniel Sanghoon Shin, Jesse Zaretsky, et al.

Cancer Immunol Res 2016;4:194-203. Published OnlineFirst January 19, 2016.